

Ejecta and progenitor of the low-luminosity Type IIP supernova 2003Z

Victor P. Utrobin^{1,2}, Nikolai N. Chugai³, and Andrea Pastorello⁴

¹ Max-Planck-Institut für Astrophysik, Karl-Schwarzschild-Str. 1, D-85741 Garching, Germany

² Institute of Theoretical and Experimental Physics, B. Chermushkinskaya St. 25, 117218 Moscow, Russia

³ Institute of Astronomy of Russian Academy of Sciences, Pyatnitskaya St. 48, 109017 Moscow, Russia

⁴ Astrophysics Research Centre, School of Mathematics and Physics, Queen's University Belfast, Belfast BT7 1NN, United Kingdom

Received 6 September 2007 / accepted 28 September 2007

ABSTRACT

Context. The origin of low-luminosity Type IIP supernovae is unclear: they have been proposed to originate either from massive ($\sim 25 M_{\odot}$) or low-mass ($\sim 9 M_{\odot}$) stars.

Aims. We wish to determine parameters of the low-luminosity Type IIP supernova 2003Z, to estimate a mass-loss rate of the presupernova, and to recover a progenitor mass.

Methods. We compute the hydrodynamic models of the supernova to describe the light curves and the observed expansion velocities. The wind density of the presupernova is estimated using a thin shell model for the interaction with circumstellar matter.

Results. We estimate an ejecta mass of $14.0 \pm 1.2 M_{\odot}$, an explosion energy of $(2.45 \pm 0.18) \times 10^{50}$ erg, a presupernova radius of $229 \pm 39 R_{\odot}$, and a radioactive ^{56}Ni amount of $0.0063 \pm 0.0006 M_{\odot}$. The upper limit of the wind density parameter in the presupernova vicinity is $10^{13} \text{ g cm}^{-1}$, and the mass lost at the red/yellow supergiant stage is $\leq 0.6 M_{\odot}$ assuming the constant mass-loss rate. The estimated progenitor mass is in the range of $14.4 - 17.4 M_{\odot}$. The presupernova of SN 2003Z was probably a yellow supergiant at the time of the explosion.

Conclusions. The progenitor mass of SN 2003Z is lower than those of SN 1987A and SN 1999em, normal Type IIP supernovae, but higher than the lower limit of stars undergoing a core collapse. We propose an observational test based on the circumstellar interaction to discriminate between the massive ($\sim 25 M_{\odot}$) and moderate-mass ($\sim 16 M_{\odot}$) scenarios.

Key words. stars: supernovae: individual: SN 2003Z – stars: supernovae: Type IIP supernovae

1. Introduction

Type II plateau supernovae (SNe IIP) with the plateau of ~ 100 days in the light curve are believed to be an outcome of a core collapse of the $9 - 25 M_{\odot}$ stars (e.g., Heger et al. 2003). This paradigm assuming the Salpeter mass spectrum suggests that about 66% of all SNe IIP should be produced by progenitors, i.e., stars on the main sequence, in the $9 - 15 M_{\odot}$ range. At present this general picture remains unconfirmed. It could be verified via the determination of ejecta masses from the hydrodynamic modeling for a sufficiently large sample of SNe IIP. Unfortunately, only few SNe IIP have the well-observed light curves and spectra needed to reliably reconstruct the basic SN parameters. It is not therefore surprising that up to now ejecta mass has been determined using the detailed hydrodynamic simulations for only SN 1987A and SN 1999em. It is noteworthy that, from the point of view of explosion mechanism, SN 1987A is a normal SN IIP; it has the ejecta mass, the explosion energy, and the amount of ejected ^{56}Ni comparable to those of SN 1999em.

Recently an interesting subclass of SNe IIP, so called low-luminosity SNe IIP, was selected observationally (Pastorello et al. 2004). This family is characterized by luminosities, expansion velocities, and radioactive ^{56}Ni masses which are significantly lower than those of normal SNe IIP. Two views on the origin of low-luminosity SNe IIP have been proposed. Turatto et al. (1998) have suggested the origin from massive stars, $\geq 25 M_{\odot}$, which presumably form black holes and eject a low amount of ^{56}Ni ; alternatively, these SNe might originate from low-mass stars, $\sim 9 M_{\odot}$, which are expected to eject a low amount of ^{56}Ni (Chugai & Utrobin 2000; Kitaura et al. 2006).

The investigation of the origin of these SNe IIP began with some confusion. The point is that SN 1997D, the first low-luminosity SN IIP, was detected long after the explosion and, therefore, was erroneously claimed to possess a short (~ 50 days) plateau (Turatto et al. 1998). This, in turn, provoked a conclusion that SN 1997D originated from a low-mass ($\sim 9 M_{\odot}$) main-sequence star (Chugai & Utrobin 2000). The subsequent discovery of several low-luminosity SNe IIP with a long plateau of ~ 100 days (Pastorello et al. 2004) falsified this conclusion. Until now there were no attempts to model hy-

hydrodynamically low-luminosity SNe IIP on the basis of new observational data. The estimate of the ejecta masses of low-luminosity SN 1999br and SN 2003Z was made only using a semi-analytical model (Zampieri et al. 2003; Zampieri 2005). The semi-analytical model, being a sensible tool for the first order estimates, cannot, however, substitute the hydrodynamic simulations.

In this paper we study the well-observed low-luminosity Type IIP SN 2003Z (Pastorello 2003; Knop et al. 2007). Our approach is based on the hydrodynamic modeling of the light curves and expansion kinematics. This paper is organized as follows. The observational data are presented in Sect. 2. Section 3 describes the modeling procedure. Results, specifically, the SN 2003Z parameters and progenitor mass are presented in Sect. 4. The implications of the results are discussed in Sect. 5.

A distance to SN 2003Z of 21.68 Mpc is adopted using the Hubble constant $H_0 = 70 \text{ km s}^{-1} \text{ Mpc}^{-1}$ and a recession velocity of the host galaxy NGC 2742 $v_{\text{cor}} = 1518 \text{ km s}^{-1}$, corrected for the Local Group infall to the Virgo cluster and taken from the Lyon Extragalactic Data base. There are no observational signatures of the interstellar absorption in the host galaxy (Pastorello 2003) so a total extinction is taken to be equal to the Galactic value $A_B = 0.167$ (Schlegel et al. 1998).

2. Observational data

SN 2003Z was discovered very young, and a detection limit obtained nine days before the discovery allows us to constrain the explosion epoch very well, with an uncertainty of only a few days (Boles et al. 2003). We adopt an explosion date of SN 2003Z to be JD 2452665. The spectroscopic and photometric monitoring of SN 2003Z started relatively late, about 3 weeks after the discovery, and most of data were collected at the 3.5 m Telescopio Nazionale Galileo in La Palma (Spain) and the 1.82 m Copernico Telescope in Asiago (Italy). The plateau phase is quite well sampled (also thanks to the amateur's data), and a few additional data were collected during the post-plateau phase. All data have been reduced using IRAF tasks¹. In particular, photometric measurements were performed using the point spread function fitting technique. The SN magnitudes were then computed with reference to a sequence of stars in the SN vicinity, and the photometric zero-points of the different nights were obtained from observations of several standard fields (Landolt 1992). The detailed description of the data reduction techniques can be found in Pastorello et al. (2007). All observational data of SN 2003Z, first presented in Pastorello (2003), will be extensively analyzed in a forthcoming paper.

3. Model overview

A numerical modeling of SNe IIP exploits radiation hydrodynamics in the one-group approximation (Utrobin 2004). When

applied to SN 1999em (Utrobin 2007), the code results in the basic SN parameters similar to those recovered in the hydrodynamics with the multi-group approach (Baklanov et al. 2005). This suggests that the results of our modeling are not hampered by one-group approximation of the radiation transfer.

The presupernova (pre-SN) structure is set as a non-evolutionary red supergiant (RSG) star in hydrostatic equilibrium. The adopted composition of the hydrogen envelope is solar. We admit a mixing between the helium core and the hydrogen envelope similar to that in SN 1987A and SN 1999em (Utrobin 2005, 2007). The model explosion is initiated by a supersonic piston applied to the bottom of the stellar envelope outside the collapsing $1.4 M_{\odot}$ core. The time scale for the piston action is $\sim 10^{-3}$ sec. The explosion energy E is defined as a difference between the total energy input and the modulus of the binding energy of the envelope outside the collapsing core. Since in SNe IIP the radiated energy is small compared to the explosion energy, the kinetic energy of the freely expanding ejecta is practically equal to the explosion energy.

The strategy of the search for the optimal model is based on the specific dependence of the SN light curve and expansion velocities on the model parameters (cf. Utrobin 2007). The ^{56}Ni mass is determined by the bolometric luminosity of the radioactive tail, while the plateau duration, the plateau luminosity, and the velocity at the photosphere depend on the combined effects of the ejecta mass, the explosion energy, and the pre-SN radius. Specifically, the larger ejecta mass results in the longer plateau and the lower plateau luminosity; the larger explosion energy leads to the higher plateau luminosity and the shorter plateau; the larger pre-SN radius results in the higher plateau luminosity and the longer plateau. The extent of the ^{56}Ni and helium mixing also affects the light curve, particularly the shape of the plateau at the end of the photospheric epoch (Utrobin 2007). We emphasize the role of the maximal velocity of ejecta in the constraining of the model, because the density in the outermost layers is sensitive to SN parameters (Utrobin & Chugai 2005). Furthermore, the effect of a deceleration of outer layers due to the ejecta/wind interaction will be used to estimate the pre-SN wind density as was done earlier for SN 1999em (Chugai et al. 2007).

We rely on the photometric and spectroscopic data reported by Pastorello (2003). Although the hydrodynamic model reproduces the V , R , and I light curves satisfactorily, the code with one-group radiation transfer is focused on the modeling of the bolometric light curve. The observed bolometric light curve of SN 2003Z is recovered from $BVRI$ photometry using the black body approximation for the SN radiation and the standard filter responses. This suggests the determination of the radius of the SN photosphere R_{ph} and the effective temperature T_{eff} applying a minimization procedure to the errors between the observed and calculated filter responses for the adopted distance and the reddening. The bolometric luminosity is then calculated as $L = 4\pi R_{\text{ph}}^2 \sigma T_{\text{eff}}^4$, where σ is the Stephan-Boltzmann constant. The data on the photospheric velocity evolution are taken from the modeling of the Na I and Ba II lines and from Pastorello (2003), while the maximal velocity of ejecta, v_{max} , is estimated from the $\text{H}\alpha$ absorption profile. The spectrum on day 27.48 (Pastorello 2003) yields $v_{\text{max}} = 7500 \pm 200 \text{ km s}^{-1}$.

¹ IRAF is distributed by the National Optical Astronomy Observatories, which are operated by the Association of Universities for Research in Astronomy, Inc., under cooperative agreement with the National Science Foundation.

Table 1. Physical parameters of hydrodynamic models.

Model	R_0 (R_\odot)	M_{env} (M_\odot)	E (10^{50} erg)	M_{Ni} ($10^{-3} M_\odot$)	M_{He} (M_\odot)
Opt	229	14	2.45	6.28	3.9
He8	229	14	2.45	6.28	8.0
Rms	195	14	2.45	6.28	3.9
Rps	263	14	2.45	6.28	3.9
Mms	229	12	2.45	6.28	3.9
Mps	229	16	2.45	6.28	3.9
Ems	229	14	2.10	6.28	3.9
Eps	229	14	2.80	6.28	3.9
Nms	229	14	2.45	5.34	3.9
Nps	229	14	2.45	7.22	3.9

The same value we derive from the spectrum on day 9 (Knop et al. 2007). This indicates a very weak deceleration of the SN outer layers between these epochs.

4. Results

4.1. Optimal model

An extensive search in the SN parameter space led us to the optimal model of SN 2003Z (model Opt in Table 1) with the ejecta mass $M_{env} = 14 M_\odot$, the explosion energy $E = 2.45 \times 10^{50}$ erg, the ^{56}Ni mass $M_{Ni} = 0.0063 M_\odot$, and the pre-SN radius $R_0 = 229 R_\odot$. The initial density distribution in the model Opt mimics a heterogeneous structure of the RSG with the dense metal/helium core and the extended hydrogen envelope (Fig. 1). The helium core is mixed with the hydrogen envelope

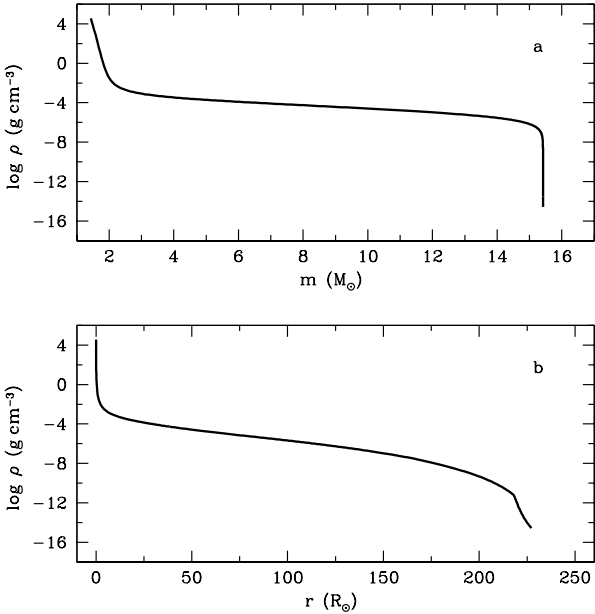


Fig. 1. Density distribution with respect to interior mass (a) and radius (b) for the optimal pre-SN model. The central core of $1.4 M_\odot$ is omitted.

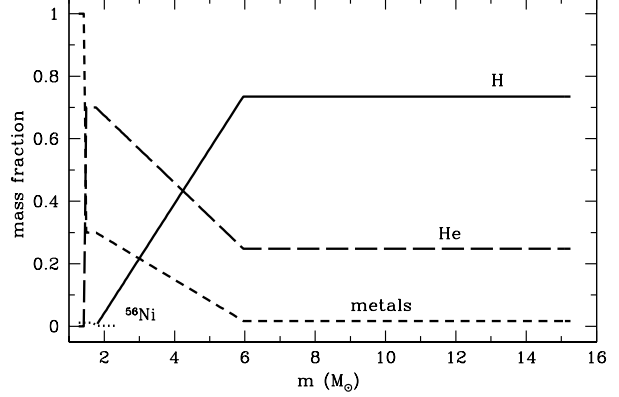


Fig. 2. The mass fraction of hydrogen (solid line), helium (long dashed line), heavy elements (short dashed line), and radioactive ^{56}Ni (dotted line) in the ejecta of the optimal model.

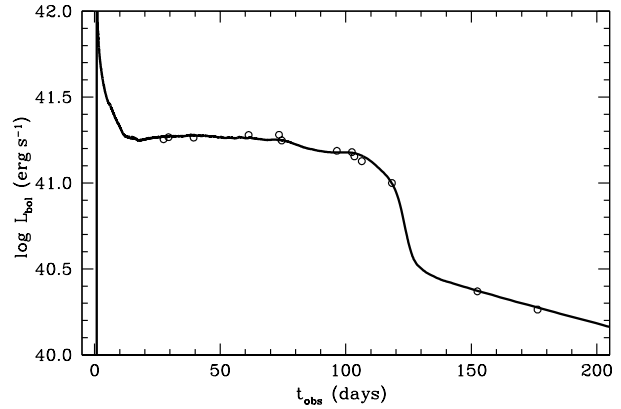


Fig. 3. Comparison of the calculated bolometric light curve of model Opt (solid line) with the bolometric data of SN 2003Z evaluated from the photometric observations of Pastorello (2003) (open circles).

so that the helium abundance drops linearly along the mass coordinate in the mixing zone (Fig. 2). In this description the mixing extent is specified by the mass coordinate of zero hydrogen abundance ($1.8 M_\odot$). Of note, SN 2003Z similar to previously studied SN 1987A and SN 1999em, requires extended mixing between the helium core and hydrogen envelope.

The bolometric light curve of SN 2003Z is fairly well fitted by the optimal model (Fig. 3). Both empirical and calculated V and R light curves (Figs. 4a and 4b) show an initial peak related to the cooling of hot outer layers of shocked ejecta. The amplitude and width of this peak depend on the structure of the outermost rarefied layers of the pre-SN envelope. We did not try to search for the appropriate density structure of the outermost layers to reproduce in detail the initial optical peak indicated by the amateur observations².

The optimal model reproduces satisfactorily the evolution of the photospheric velocity (Fig. 4c). This evolution is de-

² http://www.astrosurf.com/snweb2/2003/03Z_/03Z_Meas.htm

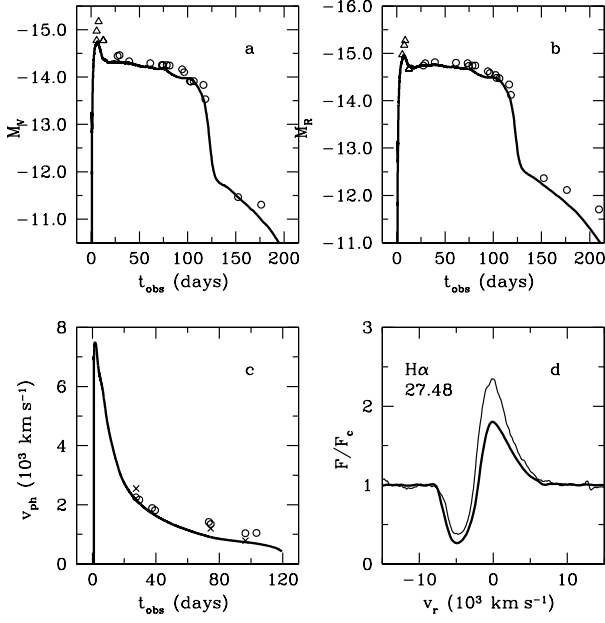


Fig. 4. Optimal hydrodynamic model. Panel (a): the calculated V light curve (solid lines) compared with the observations of SN 2003Z obtained by Pastorello (2003) (open circles) and Gary (2003) (open triangles). Panel (b): the same as panel (a) but for the R light curves. Panel (c): calculated photospheric velocity (solid line) is compared with photospheric velocities estimated from modeling the Na I doublet and Ba II 6142 Å profiles (crosses) and absorption minima of the Sc II 6246 Å line measured by Pastorello (2003) (open circles). Panel (d): $H\alpha$ profile, computed with the time-dependent approach (thick solid line), overplotted on the observed profile on day 27.48, as obtained by Pastorello (2003) (thin solid line).

terminated primarily by the density distribution in the ejecta. Remarkably, the power low density distribution in the outer layers $\rho \propto v^{-n}$ with $n = 9.2$ (Fig. 5) is very close to that with the power index $n = 9$ preferred by Knop et al. (2007) on the basis of the analysis of the early spectra. The model must also reproduce the maximal velocity $v_{\max} = 7500 \pm 200 \text{ km s}^{-1}$ derived from the blue wing of the $H\alpha$ absorption in the spectrum on day 27.48. This means that the initial velocity v_s of the boundary shell, which forms because of the radiative damping of the shock wave (Grassberg et al. 1971; Chevalier 1981), should satisfy the inequality $v_s \geq v_{\max}$. In the optimal model the boundary dense shell with the mass $M_s = 1.8 \times 10^{-4} M_\odot$ is seen in the density distribution at the velocity $v_s = 7540 \text{ km s}^{-1}$ (Fig. 5) which meets the above inequality. It is of note that we failed to find a good hydrodynamic model of SN 2003Z with the larger boundary velocity, $v_s > 7540 \text{ km s}^{-1}$. This consideration emphasizes the role of the maximal velocity of ejecta in the constraining of the hydrodynamic model.

We calculated the $H\alpha$ line on day 27.48 in the optimal model taking into account time-dependent effects of the hydrogen ionization and excitation (Utrobin & Chugai 2005). The calculated profile reproduces the blue wing of the absorption fairly well (Fig. 4d) although the model is not as good in the

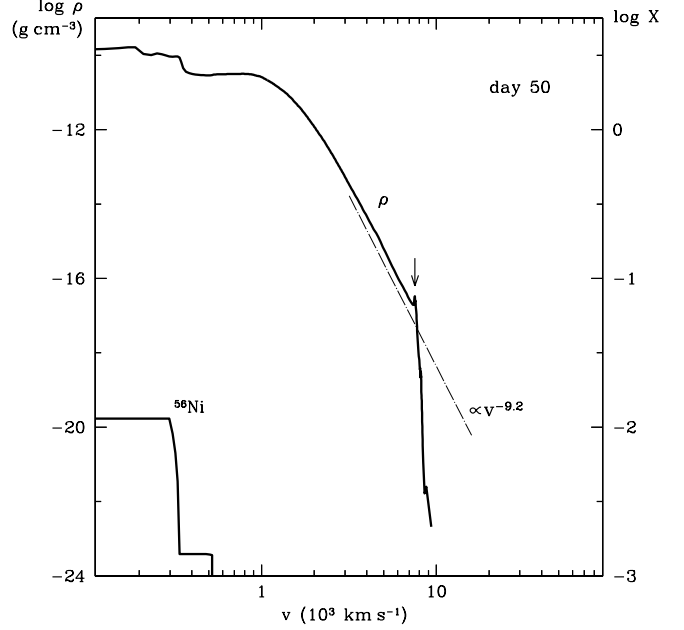


Fig. 5. The density and the ^{56}Ni mass fraction as a function of the velocity for model Opt at $t = 50$ days. Dash-dotted line is the density distribution fit $\rho \propto v^{-9.2}$. The arrow marks the boundary dense shell at the velocity $v_s = 7540 \text{ km s}^{-1}$.

emission. However, the latter is of minor importance for our purpose, the diagnostic of the density in outer layers. Indeed, the absorption depth in the blue wing of the $H\alpha$ line is determined primarily by the optical depth which, in the time-dependent approach, is a function of density in the outer layers. The fit of the calculated profile to the observations in the blue absorption wing therefore strongly supports the optimal model of SN 2003Z. The origin of the disagreement in the emission component was studied previously for SN 1987A (Utrobin & Chugai 2005) and it was found to be related to our simplified description of the ultraviolet spectrum in the range of $h\nu > 3.4 \text{ eV}$.

The last column in Table 1 is the total mass of the helium core; the value of $3.9 M_\odot$ adopted in the optimal model corresponds to a $15 M_\odot$ progenitor without rotation (Heger et al. 2000). The accurate value of the helium core mass is of little significance for the optimal model because the results are not sensitive to the helium core in a rather broad mass range. A weak sensitivity to the helium core mass has its dark side, because it prevents us from recovering the progenitor mass on the basis of only the hydrodynamic modeling. In this regard it would be of interest to consider the case of a pre-SN with a massive helium core of $8 M_\odot$ (model He8 in Table 1) which is expected for the $\approx 25 M_\odot$ progenitor without rotation (Heger et al. 2000). The helium core in this model is strongly mixed similar to the optimal model (Fig. 6a). Although the light curve of model He8 deviates from that of the optimal model (Fig. 6b), the difference is small. We believe that with a more sophisticated distribution of the mixed helium and radioactive ^{56}Ni one could reach a closer resemblance to the optimal model. This consideration indicates that a massive pro-

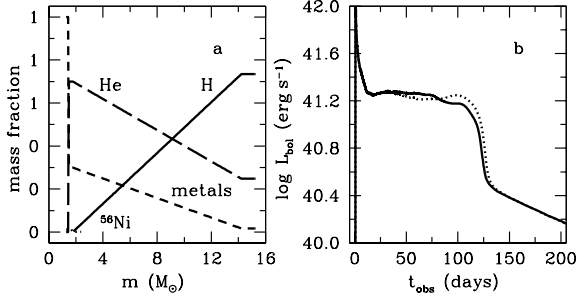


Fig. 6. Dependence on the mass of the helium core. Panel (a): the chemical composition of model He8 that differs from model Opt in the mass fraction of hydrogen (*solid line*), helium (*long dashed line*), and heavy elements (*short dashed line*), the distribution of radioactive ^{56}Ni (*dotted line*) being the same. Panel (b): bolometric light curve of model Opt (*thick solid line*) is compared with that of model He8 (*dotted line*).

Table 2. Observed parameters of auxiliary hydrodynamic models.

Model	Δt (days)	$\log L_{bol}^p$ (erg s^{-1})	v_{ph}^p (km s^{-1})	v_s (km s^{-1})
Opt	121.51	41.2643	1117.7	7540
Rms	120.90	41.1713	1052.2	8095
Rps	124.60	41.3429	1162.5	7497
Mms	118.58	41.2858	1132.4	8045
Mps	127.52	41.2306	1065.4	6972
Ems	126.74	41.2047	1025.7	6963
Eps	117.32	41.3259	1224.2	8122
Nms	118.86	41.2650	1145.6	7565
Nps	123.81	41.2614	1102.2	7573

genitor ($25 - 30 M_{\odot}$) for SN 2003Z cannot be precluded on the basis of only the hydrodynamic modeling. Note that the ejecta mass for the high-mass scenario should be $14 M_{\odot}$, so the star must lose $\Delta M \approx 10 M_{\odot}$ via the stellar wind, presumably at the RSG stage during $t_{\text{RSG}} \approx 4 \times 10^5 \text{ yr}$ (Heger 1998) with a high mass-loss rate $\dot{M} = \Delta M / t_{\text{RSG}} \approx 2.5 \times 10^{-5} M_{\odot} \text{ yr}^{-1}$. This provides us a way to verify the high-mass progenitor using the estimate of the wind density around the pre-SN in the combination with the hydrodynamic model.

The confidence in the derived model parameters is determined by the errors in the distance, the extinction, the plateau duration, and the velocity at the photosphere. Unfortunately, the errors of the SN 2003Z data are not well defined. Although the internal accuracy of the photometric data and the velocity measurements is better than 5% (Pastorello 2003), the luminosity error is certainly larger because of uncertainties in the distance and the extinction, while the photospheric velocity measured from spectral lines and the calculated photospheric velocity may refer to physically different layers. We therefore adopt rather arbitrarily, the following relative errors: 10% in the bolometric luminosity, 5% in the photospheric velocity, and 5% in the plateau duration. Note that the uncertainty of the ^{56}Ni mass is determined by the error in the bolometric luminosity. At first

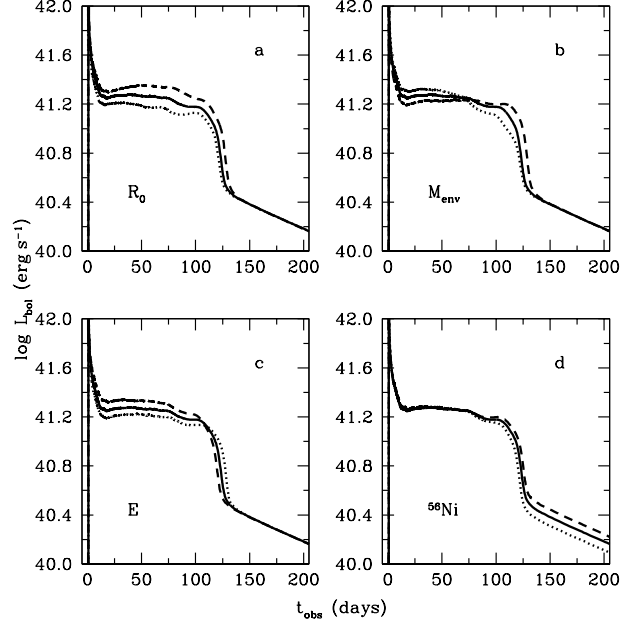


Fig. 7. Dependence of the bolometric light curve of the optimal model (*solid line*) on the basic parameters: (a) the initial radius, model Rms (*dotted line*) and model Rps (*dashed line*); (b) the ejecta mass, model Mms (*dotted line*) and model Mps (*dashed line*); (c) the explosion energy, model Ems (*dotted line*) and model Eps (*dashed line*); (d) the total ^{56}Ni mass, model Nms (*dotted line*) and model Nps (*dashed line*).

glance the error in the luminosity is underestimated, since the error in the distance could be as large as 10% (or 20% in luminosity) given possible uncertainties in the Hubble constant and in the corrected recession velocity of NGC 2742. On the other hand, our extensive modeling shows that in order to reproduce both the observed maximal ejecta velocity and the light curve, one needs to adopt the maximal distance to NGC 2742 (21.68 Mpc). No much room, therefore, is left for the distance variation. This justifies our choice for the luminosity error.

Using the auxiliary models (Tables 1 and 2, Fig. 7), we are able to translate the adopted errors of the observational parameters into the uncertainties in the pre-SN radius of $\pm 39 R_{\odot}$, the ejecta mass of $\pm 1.2 M_{\odot}$, the explosion energy of $\pm 0.18 \times 10^{50} \text{ erg}$, and the ^{56}Ni mass of $\pm 0.0006 M_{\odot}$. The ejecta mass thus turns out to be in the range $12.8 - 15.2 M_{\odot}$. Amazingly, using the semi-analytical model, Zampieri (2005) found that the ejecta of SN 2003Z lies in the range $13 - 19 M_{\odot}$ which is very close to our result. With the adopted errors, the pre-SN mass (ejecta plus neutron star) falls into the $14.2 - 16.6 M_{\odot}$ range.

4.2. Progenitor

The small difference between the computed boundary shell velocity of 7540 km s^{-1} and the observed maximal velocity on day 27.48 of $7500 \pm 200 \text{ km s}^{-1}$ places a large constraint on the pre-SN wind density: the absence of the pronounced ejecta deceleration during the first 27 days implies that the wind should

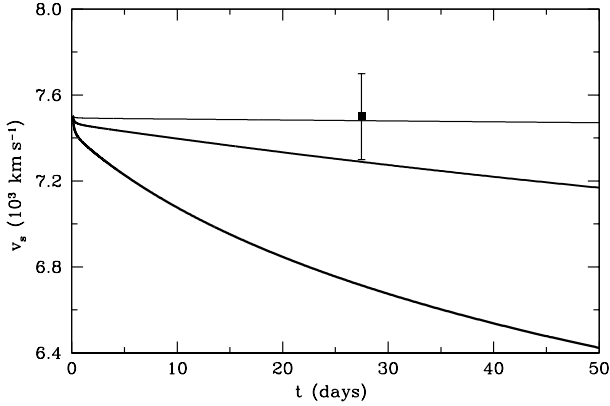


Fig. 8. Evolution of the maximal velocity of the ejecta in the optimal model for three values of dimensionless wind density parameter ω : 1 (*thick line*), 0.15 (*medium line*), and 0.01 (*thin line*). The observed maximal velocity with the corresponding uncertainty is shown on day 27.48.

not be very dense. To find an upper limit of the wind density parameter $w = \dot{M}/u$ (where u is the wind velocity), we compute the deceleration of the outer layers of the model ejecta assuming the thin shell approximation (Chugai et al. 2007). We introduce for convenience the dimensionless parameter $\omega = w/w_1$ where $w_1 = 6.3 \times 10^{13} \text{ g cm}^{-1}$; the latter corresponding, for example, to the combination of $\dot{M} = 10^{-6} M_{\odot} \text{ yr}^{-1}$ and $u = 10 \text{ km s}^{-1}$. The calculated evolution of the maximal velocity of the SN 2003Z ejecta for the optimal model is shown in Fig. 8 for three cases: $\omega = 1, 0.15$, and 0.01 . The case $\omega = 1$ predicts a too strong deceleration and should be discarded. The wind with $\omega = 0.15$ is barely consistent with the observed maximal velocity within the error. We thus conclude that the density parameter for the pre-SN wind of SN 2003Z is $\omega \leq 0.15$ or $w \leq 10^{13} \text{ g cm}^{-1}$ in CGS units.

Another look at the wind density issue could be provided by the analysis of the contribution of the circumstellar interaction to the late time luminosity of SN 2003Z. Unfortunately, the photometry for this SN is limited by the age of ≈ 200 days at which only a high upper limit for the density of the circumstellar matter can be derived. We can consider, however, SN 1997D, another low-luminosity SN IIP, which does not show signatures of the circumstellar interaction in the light curve till day 400 (Benetti et al. 2001). This suggests the absence of a dense circumstellar medium around this SN. We can use the circumstellar interaction model (Chugai et al. 2007) to quantify this statement. Given the similarity of SN 1997D and SN 2003Z we use the ejecta mass and kinetic energy of SN 2003Z to estimate the upper limit of the wind density parameter $w \sim 6 \times 10^{14} \text{ g cm}^{-1}$ for SN 1997D. It is natural to admit that a similar wind is characteristic of the SN 2003Z environment as well. This upper limit, however, is of little interest in the context of SN 2003Z because it is 60 times higher than that obtained above from the early time ejecta deceleration.

The wind density parameter of SN 2003Z estimated from the ejecta deceleration is at least seven times lower than that

for the normal Type IIP SN 1999em (Chugai et al. 2007). Assuming that the wind velocities of both pre-SNe are comparable we conclude that the mass-loss rate in the case of SN 2003Z is at least seven times lower than that of SN 1999em. Given that the mass-loss rate increases with the progenitor mass (Neuwenhujzen & de Jager 1990) the difference in the wind density implies that the progenitor of SN 2003Z is less massive compared to that of SN 1999em.

In order to convert the pre-SN mass into the progenitor mass, requires knowledge of the mass lost via the stellar wind on the main sequence and at the RSG stage. The mass lost on the main sequence for the $\sim 15 M_{\odot}$ star is $\sim 0.2 M_{\odot}$ (cf. Heger et al. 2000), while at the RSG stage the lost mass is $\Delta M = t_{\text{RSG}} w u$, where $t_{\text{RSG}} \sim 10^6 \text{ yr}$ is the duration of the RSG stage for the $\sim 15 M_{\odot}$ star (Heger 1998). The wind velocity is a poorly known parameter. For the RSG stars the velocity is in the range of $10 - 40 \text{ km s}^{-1}$ (Cherchneff & Tielens 1994). However, the pre-SN of SN 2003Z with the radius of $229 R_{\odot}$ seems to be closer to a yellow supergiant (YSG). Indeed, for the $15 M_{\odot}$ star luminosity of $L \approx 6 \times 10^4 L_{\odot}$ (Heger et al. 2000), the effective temperature of the pre-SN of SN 2003Z would be $T_{\text{eff}} \approx 6000 \text{ K}$, i.e., typical for a YSG. The wind velocities estimated from the YSG observations fall into the range of $30 - 40 \text{ km s}^{-1}$ (Lobel et al. 2003; Robberto et al. 1993). With the maximal velocity $u = 40 \text{ km s}^{-1}$ the mass-loss rate immediately before the explosion is $\dot{M} \leq 0.6 \times 10^{-6} M_{\odot} \text{ yr}^{-1}$. We assume that the mass-loss rate during the whole RSG/YSG stage is constant on average in agreement with the general wisdom that the value of \dot{M} is mainly determined by the stellar mass and luminosity (Neuwenhujzen & de Jager 1990). The mass lost at the RSG/YSG stage is then $\leq 0.6 M_{\odot}$. Adopting the mass of $0.2 M_{\odot}$ to be lost on the main sequence, we conclude that the progenitor lost $0.2 - 0.8 M_{\odot}$ owing to the wind. Combined with the pre-SN mass of $15.4 \pm 1.2 M_{\odot}$ this implies the progenitor mass of SN 2003Z to be in the range of $14.4 - 17.4 M_{\odot}$ with the average value of $\approx 16 M_{\odot}$.

5. Discussion and conclusions

The goal of this study was to recover the basic parameters of SN 2003Z and to get an idea about progenitor masses of low-luminosity SNe IIP. We estimated the ejecta mass to be $14.0 \pm 1.2 M_{\odot}$, the explosion energy $(2.45 \pm 0.18) \times 10^{50} \text{ erg}$, the pre-SN radius $229 \pm 39 R_{\odot}$, and the ^{56}Ni mass $0.0063 \pm 0.0006 M_{\odot}$. Using the ejecta/wind interaction model, we found the upper limit of the density parameter of the pre-SN wind and, assuming the constant mass-loss rate at the RSG/YSG stage, constrained the progenitor mass by the range of $14.4 - 17.4 M_{\odot}$. The estimate of the wind density thus allows us to avoid the uncertainty in the progenitor mass stemming from the weak sensitivity of the hydrodynamic model to the helium core mass.

The only normal SN IIP, studied in a similar way to SN 2003Z, is SN 1999em. Its pre-SN radius is $\approx 500 R_{\odot}$, the ejecta mass is $\approx 19 M_{\odot}$, the explosion energy is $\approx 1.3 \times 10^{51} \text{ erg}$, and the ^{56}Ni mass is $\approx 0.036 M_{\odot}$ (Utrobin 2007), while the progenitor mass is $\approx 22 M_{\odot}$ (Chugai et al. 2007). A comparison of SN 2003Z with SN 1999em taken together with the fact that the low-luminosity SNe IIP are very similar indicates

Table 3. Hydrodynamic models for SN 1987A, SN 1999em, and SN 2003Z.

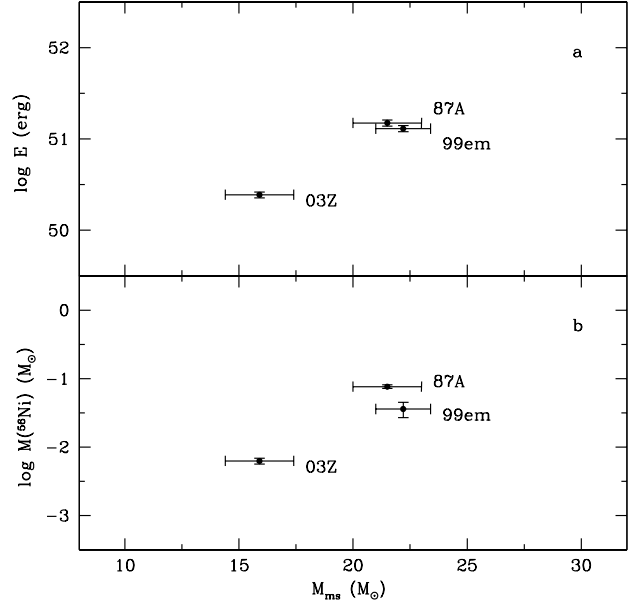
SN	R_0 (R_\odot)	M_{env} (M_\odot)	E (10^{51} erg)	M_{Ni} ($10^{-2} M_\odot$)	v_{Ni}^{max} (km s^{-1})	v_H^{min} (km s^{-1})	M_{ms} (M_\odot)
87A	35	18	1.5	7.65	3000	600	21.5
99em	500	19	1.3	3.60	660	700	22.2
03Z	229	14	0.245	0.63	535	360	15.9

that this variety of SNe IIP originates from less massive progenitors than normal SNe IIP. Parameters of three SNe IIP — SN 1987A (Utrobin 2005), SN 1999em (Utrobin 2007; Chugai et al. 2007), and SN 2003Z (Table 3) — determined on the basis of the similar hydrodynamic modeling, suggest a picture in which ordinary SNe IIP originate from massive progenitors around $20 M_\odot$, while low-luminosity SNe IIP originate from less massive progenitors around $\sim 16 M_\odot$, close to the average mass of the $9 - 25 M_\odot$ range traditionally associated with SNe IIP. If our result for SN 2003Z is correct, then the explosion energy and the amount of ejected ^{56}Ni should significantly increase for the progenitors between $\sim 16 M_\odot$ and $\sim 20 M_\odot$ (Fig. 9). Interestingly, the empirical correlation between the explosion energy and the ^{56}Ni mass for normal SNe IIP has been demonstrated by Nadyozhin (2003). It should be emphasized that these correlations, valid for SNe IIP, may not be applicable to other SNe II. At least SN 1994W (Type IIn event) was found to have a low amount of ejected ^{56}Ni , $\sim 0.015 M_\odot$, but a normal explosion energy, $\approx 1.3 \times 10^{51}$ erg (Chugai et al. 2004).

Two alternative conjectures about the origin of low-luminosity SNe IIP have been proposed: (1) progenitors are massive stars, $\geq 25 M_\odot$ (Turatto et al. 1998); (2) these SNe originate from low-mass stars, $\sim 9 M_\odot$ (Chugai & Utrobin 2000; Kitaura et al. 2006). The present estimate of the progenitor mass of SN 2003Z, $14.4 - 17.4 M_\odot$, is in the disparity with both the high-mass and low-mass scenarios.

Our estimate of the progenitor mass is essentially based on the assumption that the mass-loss rate at the RSG/YSG stage was constant. In fact, the derived wind density refers to the close vicinity of SN 2003Z $r < R_w = vt \sim 10^{16}$ cm (where $v \approx 7 \times 10^8$ cm s $^{-1}$ is the SN expansion velocity in the outer layers and $t \sim 10^7$ sec is the characteristic age of the SN). This linear scale with the wind velocity $u > 10$ km s $^{-1}$ corresponds to the wind history during the latest $R_w/u < 300$ yr before the explosion. Most of the RSG/YSG stage, i.e. $4 \times 10^5 - 10^6$ yr, is thus hidden from our sight. One might suggest that the mass-loss rate was substantially more vigorous in the past than immediately before the SN explosion. If this questionable possibility were the case, the $25 M_\odot$ progenitor would lose $\sim 10 M_\odot$, and the high-mass scenario for SN 2003Z would be saved. Of note, the essentially higher wind density of pre-SN in this case suggests that the dense wind at the large radii could be revealed via radio and X-ray observations at the large age, $t \geq 10$ yr.

A remarkable property of all three SNe is strong mixing between the helium core and the hydrogen envelope indicated by a low minimal velocity of hydrogen matter (Table 3). Generally, the model with the unmixed helium core shows

**Fig. 9.** Explosion energy (a) and ^{56}Ni mass (b) versus progenitor mass for three core-collapse SNe.

a bump in the light curve at the end of the plateau (Utrobin 2007); the absence of the bump in the available light curves of SNe IIP, in addition to the narrow-topped H α emission at the nebular phase, indicates that substantial mixing between the helium core and the hydrogen envelope is a universal phenomenon for SNe IIP. This mixing could be induced by the convection during the growth of helium core (Barkat & Wheeler 1988) or/and during the SN explosion (Kifonidis et al. 2006).

It is noteworthy that the radii of all three pre-SNe IIP (Table 3) are notably lower than a radius of typical massive RSG, e.g., the radius of $\approx 800 R_\odot$ for α Ori (Harper et al. 2001). We have already shown that the SN 2003Z pre-SN was the YSG rather than the RSG. For SN 1999em the $22 M_\odot$ pre-SN with the luminosity of $\approx 10^5 L_\odot$ is characterized by the effective temperature of ~ 4700 K, which is intermediate between the RSG and YSG values. Interestingly, the pre-SN of SN 2004et, a normal SN IIP, was probably a YSG as well (Li et al. 2005). These cases suggest that not only the pre-SN 1987A, but a possibly significant fraction of pre-SNe IIP, experience an excursion on the Hertzsprung-Russell (HR) diagram from the RSG towards the YSG before the explosion. Note, some pre-SNe IIP, when becoming the YSG, could get into the instability strip and manifest themselves before the explosion as long period ($P \sim 50 - 100$ days) Cepheids. If this is the case, the recovery of the Cepheid period of a pre-SN on the basis of a set of pre-explosion observations could provide us with an additional tool for the mass determination from the pulsation period.

The recovered progenitor mass of SN 2003Z raises a crucial question: what happens to the $9 - 15 M_\odot$ stars which make up $\approx 66\%$ of all the stars from the $9 - 25 M_\odot$ mass range. Two conceivable suggestions are: (A) all the $9 - 15 M_\odot$ stars explode as low-luminosity, or even fainter, SNe IIP; (B) low-luminosity SNe IIP originate only from a narrow range of pro-

genitors around $\sim 16 M_{\odot}$, while the rest of the $9 - 15 M_{\odot}$ stars produce different varieties of SNe II. A large sample of SNe II which is well observed and studied is certainly needed to distinguish between the options A and B. It should be emphasized that the initial peak, the end of the plateau, and the radioactive tail are of crucial importance for the recovery of reliable SN II parameters.

An alternative approach to determine the pre-SN mass exploits archival pre-explosion images of host galaxies and stellar evolution tracks on the HR diagram. Interestingly, using the archival HST images Van Dyk et al. (2003) and Maund & Smartt (2005) derived an upper limit of $\sim 15 M_{\odot}$ and $\sim 12 M_{\odot}$, respectively, for the progenitor of the low-luminosity SN 1999br. Given a similarity of known low-luminosity SNe IIP these estimates make the high-mass scenario unlikely.

It should be emphasized that a test of the mass determination method based on the pre-explosion images is needed; for instance, the pre-SN light could be partially absorbed in a dusty circumstellar envelope. In this regard it would be of top priority to determine independently the progenitor mass both from the pre-discovery images and from the hydrodynamic simulations. Among SNe IIP, except for SN 1987A, only SN 2004et and SN 2005cs were detected in the pre-discovery images (Li et al. 2005; Maund et al. 2005; Li et al. 2006) and have the light curves and spectra appropriate for the hydrodynamic modeling as well (Sahu et al. 2006; Misra et al. 2007; Pastorello et al. 2006; Tsvetkov et al. 2006). These two challenging cases require a detailed study.

Acknowledgements. VU thanks Wolfgang Hillebrandt for the excellent opportunity to work at the MPA. We thank the referee David Branch for helpful comments. This work was supported in part by the Russian Foundation for Fundamental Research (05-02-17480 and 08-02-00761).

References

- Baklanov, P. V., Blinnikov, S. I., & Pavlyuk, N. N. 2005, *Astron. Lett.*, 31, 429
- Barkat, Z., & Wheeler, J. C. 1988, *ApJ*, 332, 247
- Benetti, S., Turatto, M., Balberg, S., et al. 2001, *MNRAS*, 322, 361
- Boles, T., Beutler, B., Li, W., et al. 2003, *IAU Circ. No.* 8062
- Brown, P. J., Dessart, L., Holland, S. T., et al. 2007, *ApJ*, 659, 1488
- Cherchneff, I., & Tielens, A. G. G. M. 1994, in the 34th Herstmonceux Conf., *Circumstellar Media in Late Stages of Stellar Evolution*, ed. R. E. S. Clegg, I. R. Stevens, & W. P. S. Meikle (Cambridge, UK: Cambridge University Press), 232
- Chevalier, R. A. 1981, *Fund. of Cosmic Phys.*, 7, 1
- Chugai, N. N., & Utrobin, V. P. 2000, *A&A*, 354, 557
- Chugai, N. N., Blinnikov, S. I., Cumming, R. J., et al. 2004, *MNRAS*, 352, 1213
- Chugai, N. N., Chevalier, R. A., & Utrobin, V. P. 2007, *ApJ*, 662, 1136
- Gary, B. L. 2003, *SN Web*
- Grassberg, E. K., Imshennik, V. S., & Nadyozhin, D. K. 1971, *Ap&SS*, 10, 28
- Harper, G. M., Brown, A., & Lim, J. 2001, *ApJ*, 551, 1073
- Heger, A. 1998, *The presupernova evolution of rotating massive stars*. PhD thesis, Technische Universität München
- Heger, A., Langer, N., & Woosley, S. E. 2000, *ApJ*, 528, 368
- Heger, A., Fryer, C. L., Woosley, S. E., Langer, N., & Hartmann, D. H. 2003, *ApJ*, 591, 288
- Kifonidis, K., Plewa T., Scheck L., Janka H.-Th., & Müller, E. 2006, *A&A*, 453, 661
- Kitaura, F. S., Janka, H.-Th., & Hillebrandt, W. 2006, *A&A*, 450, 345
- Knop, S., Hauschildt, P. H., Baron, E., & Dreizler, S. 2007, *A&A*, 469, 1077
- Landolt, A. U. 1992, *AJ*, 104, 340
- Li, W., Van Dyk, S. D., Filippenko, A. V., & Cuillandre, J.-C. 2005, *PASP*, 117, 121
- Li, W., Van Dyk, S. D., Filippenko, A. V., et al. 2006, *ApJ*, 641, 1060
- Lobel, A., Dupree, A. K., Stefanik, R. P., et al. 2003, *ApJ*, 583, 923
- Maund, J. R., & Smartt, S. J. 2005, *MNRAS*, 360, 288
- Maund, J. R., Smartt, S. J., & Danziger, I. J. 2005, *MNRAS*, 364, L33
- Misra, K., Pooley, D., Chandra, P., et al. 2007, *MNRAS*, 381, 280
- Nadyozhin, D. K. 2003, *MNRAS*, 346, 97
- Nieuwenhuijzen, H., & de Jager, C. 1990, *A&A*, 231, 134
- Pastorello, A. 2003, *H-rich core-collapse supernovae*. PhD thesis, University of Padova
- Pastorello, A., Zampieri, L., Turatto, M., et al. 2004, *MNRAS*, 347, 74
- Pastorello, A., Sauer, D., Taubenberger, S., et al. 2006, *MNRAS*, 370, 1752
- Pastorello, A., Taubenberger, S., Elias-Rosa, N., et al. 2007, *MNRAS*, 376, 1301
- Robberto, M., Ferrari, A., Nota, A., & Paresce, F. 1993, *A&A*, 269, 330
- Sahu, D. K., Anupama, G. C., Srividya, S., & Muneer, S. 2006, *MNRAS*, 372, 1315
- Schlegel, D. J., Finkbeiner, D. P., & Davis, M. 1998, *ApJ*, 500, 525
- Tsvetkov, D. Yu., Volnova, A. A., Shulga, A. P., et al. 2006, *A&A*, 460, 769
- Turatto, M., Mazzali, P. A., Young, T. R., et al. 1998, *ApJ*, 498, L129
- Utrobin, V. P. 2004, *Astron. Lett.*, 30, 293
- Utrobin, V. P. 2005, *Astron. Lett.*, 31, 806
- Utrobin, V. P. 2007, *A&A*, 461, 233
- Utrobin, V. P., & Chugai, N. N. 2005, *A&A*, 441, 271
- Van Dyk, S. D., Li, W., & Filippenko, A. V. 2003, *PASP*, 115, 1289
- Zampieri, L. 2005, in "1604–2004: Supernovae as cosmological light-houses", *ASP Conf. Series*, Vol. 342, ed. M. Turatto, S. Benetti, L. Zampieri, & W. Shea (San Francisco: Astron. Soc. of the Pacific), 358
- Zampieri, L., Pastorello, A., Turatto, M., et al. 2003, *MNRAS*, 338, 711